One Step Pd(0)-Catalyzed Synthesis, X-ray Analysis, and Photophysical Properties of Cyclopent[hi]aceanthrylene: Fullerene-like Properties in a Nonalternant Cyclopentafused Aromat...

ARTICLE *in* JOURNAL OF THE AMERICAN CHEMICAL SOCIETY · JANUARY 2002

Impact Factor: 12.11 · DOI: 10.1021/ja016189b · Source: PubMed

3 AUTHORS, INCLUDING:

Marcia Levitus
Arizona State University
54 PUBLICATIONS **1,458** CITATIONS
SEE PROFILE

Miguel A Garcia-Garibay
University of California, Los Angeles
226 PUBLICATIONS **4,836** CITATIONS
SEE PROFILE

J|A|C|S
ARTICLES
Published on Web 12/08/2001

One Step Pd(0)-Catalyzed Synthesis, X-ray Analysis, and Photophysical Properties of Cyclopent[*hi*]aceanthrylene: Fullerene-like Properties in a Nonalternant Cyclopentafused Aromatic Hydrocarbon

Hung Dang, Marcia Levitus, and Miguel A. Garcia-Garibay*

Contribution from the Department of Chemistry and Biochemistry, University of California, Los Angeles, California 90095-1569

Received May 13, 2001

Abstract: A simple procedure for the synthesis of cyclopentafused polycyclic aromatic hydrocarbons (CP-PAH) with $Pd(PPh_3)_2Cl_2$ catalyst has been applied to the one-pot palladium(0)-catalyzed coupling of 9,10-dibromoanthracene (**1**) with 2-methyl-3-butyn-2-ol. Reactions carried out in refluxing benzene in the presence of $CuSO_4/Al_2O_3$ yielded 9,10-dialkynylanthracene **2a**, alkynyl aceanthrylene **2b**, and 2,7-disubstituted cyclopent[*hi*]aceanthrylene **2c** in 13%, 23%, and 19% purified yields, respectively, with total conversions of 80−90%. Sealed tube reactions without copper at 110 °C improved the yield of **2c** up to >75%. Single-crystal X-ray analyses of **2a** and **2c** reveal a three-dimensional hydrogen bonding network, producing a unique crystal packing. The packing structure of **2b** is dominated by $\pi-\pi$ stacking interactions between two aceanthrylene molecules. CP-PAHs **2b** and **2c** have potentially interesting fullerene-like photophysics. While the UV−vis and fluorescence spectra of **2a** ($\Phi_F = 0.87$) show the characteristic vibronic structure of anthracene, the UV−vis spectra of ruby-red aceanthrylene **2b** and greenish-black cyclopent[*hi*]aceanthrylene **2c** extend well into the visible range. Isomers **2b** and **2c** showed no detectable fluorescence emission. Unlike fullerenes, compounds **2b** and **2c** are poor singlet oxygen sensitizers with measured $^1O_2$ quantum yields of 0.02 and 0.06, respectively. As expected from a simple Hückel analysis, **2c** has relatively low two-electron reduction potentials as determined by cyclic voltammetry.

Introduction

Considerable efforts recently have been directed toward the synthesis and study of the nonalternant cyclopentafused class of polycyclic aromatic hydrocarbons (CP-PAHs).[1,2] Included in this class are compounds such as acenaphthylene (**Acn**), pyracylene (**Pyc**), bowl-shaped molecules such as corannulene (**Cor**), and the title compound cyclopent[*hi*]aceanthrylene (Scheme 1). Prominent among their properties are their carcinogenicity,[3,4] their structural relation to C_{60} and other fullerenes, and their remarkable optical properties, which may be responsible for visible absorption bands in interstellar clouds.[5] While the synthesis of CP-PAHs is commonly based on pyrolytic isomerization of suitable precursors,[1] we recently discovered and optimized a one-step Pd(0)-catalyzed cyclopentenelation of

Scheme 1

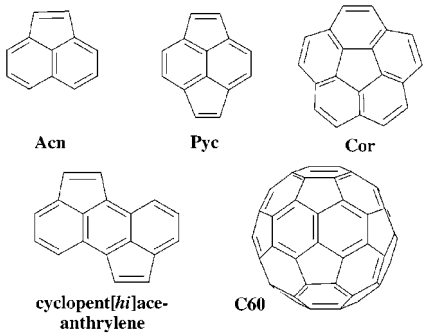

Scheme 2

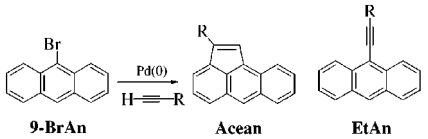

9-bromoanthracene with terminal acetylenes (Scheme 2).[6] The cyclopentenelation reaction proceeds best in benzene in a sealed tube at 110 °C in the presence of 5 mol % $Pd(PPh_3)_2Cl_2$ with 400 mol % of Et_3N.[6] Although our interest was focused on the photophysics of alkynyl-substituted arenes[7] prepared by Sono-

(1) (a) Scott, L. T. *Pure Appl. Chem.* **1996**, *68*, 291−300. (b) Necula, A.; Scott, L. T. *J. Anal. Appl. Pyrolysis* **2000**, *54*, 65−87. (c) Scott, L. T.; Bronstein, H. E.; Preda, D. V.; Ansems, R. B. M.; Bratcher, M. S.; Hagen, S. *Pure Appl. Chem.* **1999**, *71*, 209−219.
(2) (a) Rabideau, P. W.; Sygula, A. *Acc. Chem. Res.* **1996**, *29*, 235−242. (b) Borchardt, A.; Fuchicello, A.; Kilway, K. V.; Baldridge, K. K.; Siegel, J. S. *J. Am. Chem. Soc.* **1992**, *114*, 1921−1923.
(3) Sarobe, M.; Jenneskens, L. W.; Wesseling, J.; Wiersum, U. E. *J. Chem. Soc., Perkin Trans. 2* **1997**, 703−708 and references therein.
(4) (a) Lowe, J. P.; Silverman, B. D. *Acc. Chem. Res.* **1984**, *17*, 332−338. (b) Ball, L. M.; Warren, S. H.; Sangaiah, R.; Nesnow, S.; Gold, A. *Mutation Res.* **1989**, *224*, 115−125.
(5) (a) Fulara, J.; Kreowski, J. *New Astron. Rev.* **2000**, *44*, 581−597. (b) Goeres, A.; Keller, R.; Sedlmayr, E.; Gail, H. P. *Polycyclic Aromat. Compd.* **1996**, *8*, 129−165. (c) Kroto, H. W.; Heath, J. R.; O'Brien, S. C.; Curl, R. F.; Smalley, R. E. *Nature* **1985**, *318*, 162−163.
(6) Dang, H.; Garcia-Garibay, M. A. *J. Am. Chem. Soc.* **2001**, *123*, 355−356.

10.1021/ja016189b CCC: $22.00

Scheme 3 [a]

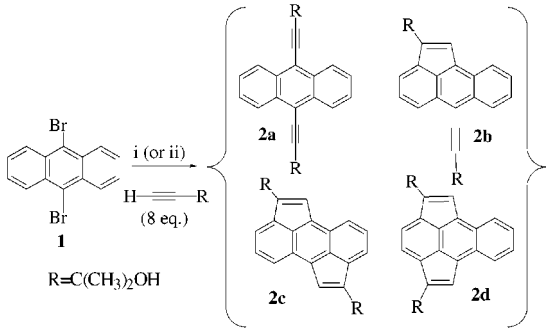

[a] Conditions: (i) $Pd(PPh_3)_2Cl_2$ (5 mol %), PPh_3 (23 mol %), Et_3N (400 mol %), $CuSO_4/Al_2O_3$, refluxing benzene, 16h. (ii) $Pd(PPh_3)_2Cl_2$ (5 mol %), PPh_3 (23 mol %), Et_3N (800 mol %), benzene, pressure tube at 110 °C, 16 h.

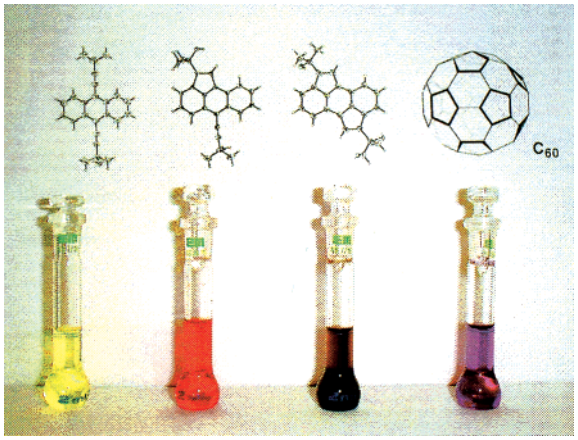

Figure 1. Dilute toluene solutions of compounds **2a**, **2b**, and **2c** illustrating the remarkable changes in UV−vis absorption spectra as a function of mono- and bis-cyclopentenelation. A dilute solution of $\mathbf{C_{60}}$ is also shown for comparison.

gashira[8] coupling, we recognized the potential of this simple variation as an ideal way to prepare other CP-PAHs. With that in mind, we analyzed the Pd(0)-catalyzed double cyclopentenelation of 9,10-dibromoanthracene with 8 equiv of 2-methyl-3-butyn-2-ol (Scheme 3). We report here a very efficient one-step formation of cyclopent[*hi*]aceanthrylene **2c** under conditions where 9,10-dialkynylanthracene **2a** and alkynyl aceanthrylene **2b** are minimized. The isomeric benzopyracylene **2d** was not observed. One of the most striking features of compounds **2a**−**c** came from their kaleidoscopic UV−vis spectral behavior (Figure 1). While compound **2a** is pale yellow and highly fluorescent, compounds **2b** and **2c** are ruby red and dark greenish-brown, respectively. A loose analogy between the UV−vis absorption spectrum of cyclopent[*hi*]aceanthrylene **2c** and C_{60}[9] led us to investigate its photophysical properties, including its $^1O_2$ sensitization abilities and electrochemical reduction. We also describe here a detailed structural analysis of compounds **2b** and **2c** by single-crystal X-ray diffraction, including a remarkably thermally stable packing structure in the case of compound **2c**.

(7) (a) Levitus, M.; Garcia-Garibay, M. A. *J. Phys. Chem.* **2000**, *104*, 8632−8637. (b) Levitus, M.; Schmieder, K.; Ricks, H.; Schimizu, K. D.; Bunz, U. H. F.; Garcia-Garibay, M. A. *J. Am. Chem. Soc.* **2001**, *123*, 4259−4265. (c) Levitus, M.; Zepeda, G.; Dang, H.; Godinez, C.; Khuong, T. A.; Schmieder, K.; Garcia-Garibay, M. A. *J. Org. Chem.* **2001**, *66*, 3188−3195.

(8) Sonogashira, K.; Tohda, Y.; Hagihara, N. *Tetrahedron Lett.* **1975**, 4467−4470.

(9) (a) Foote, C. S. *Top. Curr. Chem.* **1994**, *169*, 347−363. (b) Guldi, D. M.; Prato, M. *Acc. Chem. Res.* **2000**, *33*, 695−703.

Results and Discussion

1. Palladium(0)-Catalyzed Synthesis. The Pd(0)-catalyzed coupling of 9-bromoanthracene with monoprotected acetylenes is shown in Scheme 2.[6] Using similar reaction conditions, one-pot palladium(0)-catalyzed coupling of 9,10-dibromoanthracene (**1**) with 2-methyl-3-butyn-2-ol in the presence of $Pd(PPh_3)_2Cl_2$, PPh_3, Et_3N, $CuSO_4/Al_2O_3$, in refluxing benzene generated a mixture of 9,10-dialkynylanthracene **2a**, alkynyl aceanthrylene **2b**, and 2,7-disubstituted cyclopent[*hi*]aceanthrylene **2c** (Scheme 3). The reaction was first carried out in the presence of copper to obtain all four possible regioisomeric products from the coupling reaction. The crude reaction mixture was purified by column chromatography on silica gel (1:1 hexanes/ethyl acetate) to give **2a**, **2b**, and **2c**. At 80−90% conversion of the starting material, the yields of **2a**, **2b**, and **2c** were 13%, 23%, and 19%, respectively. Reactions in a sealed tube at 110 °C in the absence of copper (Scheme 3, ii), as reported in our previous communication, yielded compound **2c** with greater than 75% selectivity. As determined by ^1H NMR, the yields of compounds **2a** and **2b** under these conditions were ca. 20% and 5%, respectively.

Compounds **2a**, **2b**, and **2c** were crystallized from a wide variety of solvents to yield orange, ruby-red, and black crystals, respectively. All three compounds were characterized by their spectral data and by single-crystal X-ray diffraction analysis.

Anthracene **2a** and aceanthrylene **2b** have melting point ranges of 214.0−217.5 and 172.0−174.5 °C, respectively. Crystals of cyclopent[*hi*]aceanthrylene **2c** grown from methylene chloride were found to have very interesting solid-state properties that were analyzed by visual inspection and differential scanning calorimetry. While solvent of crystallization is lost upon heating at moderate temperatures, desolvated samples undergo a solid-to-solid transition at ca. 210 °C well before decomposing without melting above 400 °C.

The high efficiency of the one-step synthesis of CP-PAH **2c** offers a great practical advantage over previously reported multi-step processes[10] or flash vacuum pyrolysis (FVP),[11] which often results in low overall yields. Interestingly, in agreement with literature reports where cyclopent[*fg*]aceanthrylene was not observed from flash vacuum pyrolysis (FVP) of diethynylanthracenes,[11a] the CP-PAH **2d** was not detected in the Pd(0)-catalyzed reaction mixture. It has been predicted that formation of cyclopent[*fg*]aceanthrylene is unfavorable due to the high strain energy of the pyracylene moiety. Although cyclization of aryl acetylenes to form etheno-bridged aromatic compounds is expected to be exothermic by 15−20 kcal/mol,[12] the calculated heat of formation of cyclopent[*fg*]aceanthrylene **2d** lies very close to that of the ring-open isomer **2b**, thus isomer **2d** can disappear under FVP conditions as fast as it is formed, and the final cyclization of **2b** to **2c** (exothermic by 18−22 kcal/mol) may drive the equilibrium mixture into a low-energy minimum.[11a]

(10) (a) Becker, H.-D.; Hansen, L.; Andersson, K. *J. Org. Chem.* **1985**, *50*, 277−279. (b) Plummer, B. F.; Al-Saigh, Z. Y.; Arfan, M. *J. Org. Chem.* **1984**, *49*, 2069−2071. (c) Mulder, P. P. J.; Boerrigter, J. O.; Boere, B. B.; Zuilhof, H.; Erkelens, C.; Cornelisse, J.; Lugtenburg, J. *Recl. Trav. Chim. Pays-Bas* **1993**, *112*, 287−302. (d) Boere, B. B.; Mulder, P. P. J.; Cornelisse, J.; Lugtenburg, J. *Recl. Trav. Chim. Pays-Bas* **1990**, *109*, 463−466.

(11) (a) Scott, L. T.; Necula, A. *Tetrahedron Lett.* **1997**, *38*, 1877−1880. (b) Sarobe, M.; Snoeijer, J. D.; Jenneskens, L. W.; Zwikker, J, W.; Wesseling, J. *Tetrahedron Lett.* **1995**, *36*, 9565−9566.

(12) See ref 3 in: Scott, L. T.; Necula, A. *Tetrahedron Lett.* **1997**, *38*, 1877−1880.

The results reported by Scott and co-workers are consistent with our low-level AM1 calculations[13] on the four possible products from the Pd(0)-catalyzed coupling reaction. However, we have also found that product equilibration does not occur under the Pd(0)-catalyzed conditions, suggesting that the selectivity observed in the bis-cyclopentenelation reaction reflects kinetic rather than thermodynamic control.

The ^{1}H and ^{13}C NMR spectra of the parent aceanthrylene hydrocarbon were analyzed by Scott, Rabinovitz, and co-workers within the context of electron delocalization and aromaticity.[14] The description of the neutral hydrocarbon from magnetic resonance measurements invokes a delocalized anthracene unit and a virtually isolated etheno double bond. In a similar fashion, the magnitude of the diatropic shifts for the anthracene fragment of **2b** between 8.6 and 7.6 ppm is not matched by the signal assigned to the etheno bridge at 7.45 ppm.[14] Based on the similarity between spectra obtained with **2b** and **2c**, one may conclude that a good description of the cyclopent[*hi*]aceanthrylene system may also involve a delocalized anthracene core with two relatively isolated double bonds. This simple model is supported by bond lengths determined by single-crystal X-ray diffraction.

2. Single-Crystal X-ray Analysis. X-ray quality crystals of **2a**, **2b**, and **2c** were grown by slow evaporation from chloroform, benzene, and methylene chloride, respectively. Single crystals of each isomer were mounted on a glass fiber and diffraction data were acquired using a Mo Kα radiation source ($\lambda = 0.71073$ Å). Detailed crystallographic parameters and X-ray data tables for the three isomers (**2a**, **2b**, and **2c**)[15] are included as Supporting Information.

Figure 2 shows the molecular structure of alkynyl aceanthrylene **2b** with the displacement thermal ellipsoids drawn at the 50% probability level. Compound **2b** ($P\bar{1}$, Z = 4) crystallizes in a triclinic crystal system with two independent molecules in the asymmetric unit. Bond distances in the anthracene unit vary from 1.36 to 1.44 Å, which is within the normal range for the bond order observed in aromatic systems (1.4 ± 0.04 Å).[16] Interestingly, the C2−C3 and C1−C15 bond distances of 1.48 and 1.46 Å, respectively, are slightly outside of the previously mentioned range, suggesting that the double bond in the five-membered ring is relatively isolated. The etheno-bridged carbons produce a high degree of strain caused by larger bond angles between C1−C15−C14 and C2−C3−C4 (132.20° and 136.86°, respectively), which forces the C3−C16−C15 bond angle to be 109.97°. Although a high degree of strain is produced by the five-membered ring systems, it is interesting that the aceanthrylene core is relatively flat. The ethynyl moiety is slightly deviated from linearity as shown by the ORTEP in Figure 2.

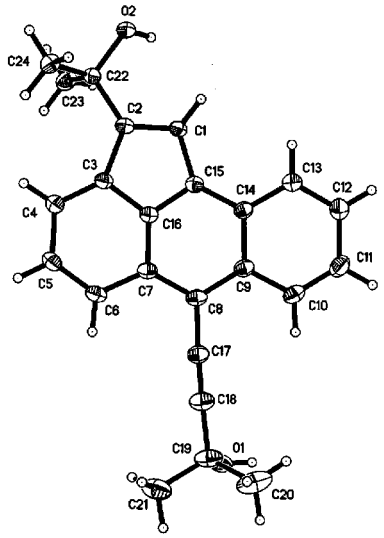

Figure 2. The molecular structure (ORTEP) of alkynyl aceanthrylene **2b** with displacement ellipsoids drawn at the 50% probability level.

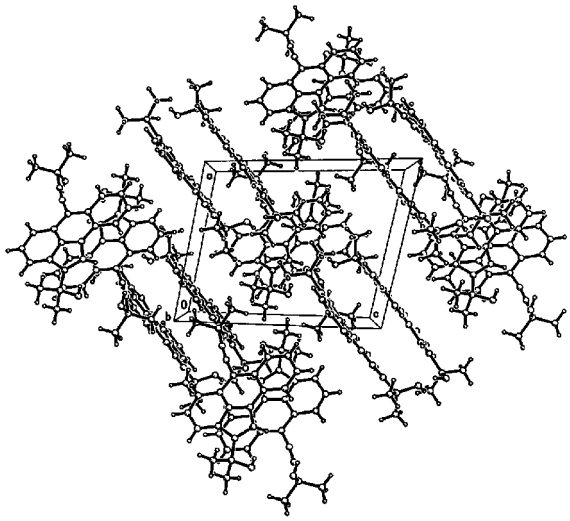

Figure 3. Crystal packing diagram of **2b** down the *b*-axis direction, illustrating $\pi-\pi$ stacking interactions between two aceanthrylene molecules.

The crystal packing diagram of isomer **2b** down the *b*-direction is shown in Figure 3. There are a total of four molecules in the unit cell, but two are related by the inversion center of the $P\bar{1}$ space group. The packing of **2b** is dominated by close $\pi-\pi$ stacking interactions between two adjacent aceanthrylene moieties. Aceanthrylene dimers pack in a centrosymmetric head-to-tail arrangement with a distance between their parallel planes of 3.729 Å. The packing structure is also characterized by pairs of molecules related to each other by a herringbone arrangement. Upon close inspection of the crystal packing, we found no close intermolecular distances between potential hydrogen bond donors and acceptors corresponding to neighboring molecules. In agreement with this observation,

(13) Heats of formation (AM1) for **2a**, **2b**, **2c**, and **2d** were calculated to be 176.0, 159.5, 141.2, and 158.0 kcal/mol, respectively.

(14) Cohen, Y.; Roelofs, N. H.; Reinhardt, G.; Scott, L. T.; Rabinovitz, M. *J. Org. Chem.* **1987**, *52*, 4207−4214.

(15) Selected crystal data: **2a**: $C_{24}H_{22}O_2$, MW = 343.43, triclinic, space group *P*1, $a = 9.161(3)$ Å, $b = 9.643(3)$ Å, $c = 12.016(4)$ Å, $\alpha = 66.720(5)°$, $\beta = 80.429(6)°$, $\gamma = 79.283(5)°$, $Z = 2$, $\rho_{calcd} = 1.193$ Mg/m^3, $F(000) = 364$, $\lambda = 0.71073$ Å^3, μ(Mo Kα) = 0.074 mm^{-1}, $T = 298(2)$ K, crystal size = 0.4 × 0.3 × 0.1 mm^3. Of the 6317 reflections collected ($1.85 \le \theta \le 28.30°$), 4374 [*R*(int) = 0.0141)] were independent reflections; max./min. residual electron density 199 and −163 e nm^{-3}, *R*1 = 0.0430 [$I > 2\sigma(I)$], and *wR*2 = 0.1376. **2b**: $C_{24}H_{22}O_2$, MW = 343.43, triclinic, space group *P*1, $a = 10.861(2)$ Å, $b = 14.303(3)$ Å, $c = 14.400(3)$ Å, $\alpha = 65.408(4)°$, $\beta = 71.975(3)°$, $\gamma = 71.561(4)°$, $Z = 4$, $\rho_{calcd} = 1.204$ Mg/m^3, $F(000) = 728$, $\lambda = 0.71073$ Å, μ(MoKα) = 0.075 mm^{-1}, $T = 100(2)$K, crystal size = 0.4 × 0.3 × 0.2 mm^3. Of the 12210 reflections collected ($1.59 \le \theta \le 28.30°$), 8578 [*R*(int) = 0.0205)] were independent reflections; max./min. residual electron density 882 and −423 e nm^{-3}, *R*1 = 0.0627 [$I > 2\sigma(I)$], and *wR*2 = 0.1818. **2c**: $C_{24}H_{22}O_2 \cdot {}^2/_3CH_2Cl_2$, MW = 399.04, trigonal, space group *P*3̄, $a = 15.6321(18)$ Å, $b = 15.6321(18)$ Å, $c = 7.2537(12)$ Å, $\alpha = \beta = 90°$, $\gamma = 120°$, $Z = 3$, $\rho_{calcd} = 1.369$ Mg/m^3, $F(000) = 662$, $\lambda = 0.71073$ Å, μ(Mo Kα) = 0.336 mm^{-1}, $T = 100(2)$ K, crystal size = 0.6 × 0.2 × 0.15 mm^3. Of the 10137 reflections collected ($1.50 \le \theta \le 28.29°$), 2494 [*R*(int) = 0.0241] were independent reflections; max./min. residual electron density 1071 and −562 e nm^{-3}, *R*1 = 0.0620 [$I > 2\sigma(I)$] ,and *wR*2 = 0.1798.

(16) (a) Julg, A.; Francoise, P. *Theor. Chim. Acta* **1967**, *8*, 249−259. (b) Baldridge, K. K.; Siegel, J. S. *J. Am. Chem. Soc.* **1992**, *114*, 9583−9587. (c) Schleyer, P. v. R.; Freeman, P. K.; Jiao, H.; Goldfuss, B. *Angew. Chem., Int. Ed. Engl.* **1995**, *34*, 337−340.

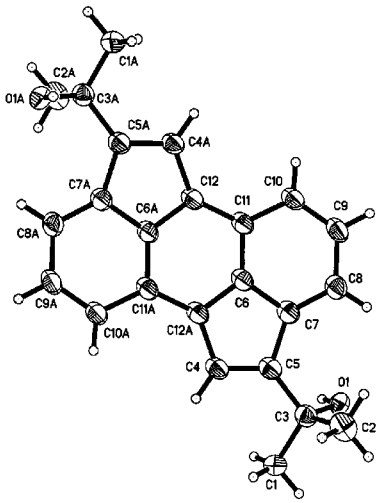

Figure 4. The molecular structure (ORTEP) of cyclopent[*hi*]aceanthrylene **2c** with displacement ellipsoids drawn at the 50% probability level.

two relatively sharp O−H stretching bands were observed at 3435 and 3337 cm^{-1} in the solid-state FT-IR spectrum.

The molecular structure of **2c** with thermal elipsoids drawn at the 50% probability level is illustrated in Figure 4. Compound **2c** crystallized in a trigonal crystal system in the space group $P\bar{3}$ with three molecules in the unit cell. Compound **2c** possesses an inversion center and the ORTEP diagram shows the atom labels from C1 to C12, with the other half related by the inversion center indicated by the labels C1A to C12A. Analysis of the C−C bond distances in **2c** revealed a similar result as that found in **2b**. Bond distances in the anthracene core fall within the typical values for condensed aromatic hydrocarbons (1.4 ± 0.04 Å). They range between 1.37 and 1.43 Å. In contrast, the bond distances between C4 to C12A and C5 to C7 were found to be 1.46 and 1.48 Å, respectively, indicating a relatively low bond order. These results indicate that the etheno-bridged carbons (C4−C5) have a small contribution to the overall aromatic delocalization. The four etheno-bridging carbons impart a high degree of strain to the cyclopentafused aceanthrylene as shown by the large bond angles C5−C7−C8 of 135.3° and C11−C12−C4A of 135.12°. In addition, the double bonds on the five-membered rings force the angle between C7−C6−C12A to be 109.6°, which is small for an sp^2 carbon atom. Remarkably, compound **2c** has no deviations from planarity.

Figure 5 illustrates the packing diagram of **2c** viewed along the *c*-axis. Isomer **2c** crystallizes with two dichloromethane molecules in the asymmetric unit. The solvent molecules are disordered about a site of crystallographic C_3 symmetry. The disordered dichloromethane molecules are located in channels parallel to the crystallographic *c*-axis. The channels are produced by unique intermolecular hydrogen bonding interactions between six molecules of **2c** as shown with dotted lines in Figure 5, which in turn are involved in hydrogen bonding with other molecules of **2c** along the *ab*-plane. At the center of the hexagonal hydrogen bonding array lies a site of crystallographic $\bar{3}$ symmetry (S_6). The packing diagram reveals strong O−H···O−H interactions, which translate along the *ab*-plane. Upon further inspection of the packing diagram of **2c**, the intimate hydrogen bonding interactions occur only across the *ab*-plane, producing layers which stack closely to create channels (down *c*-axis) where the disordered dichloromethane molecules reside

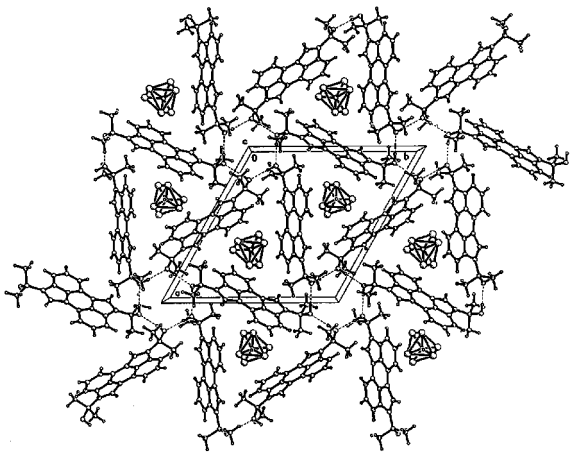

Figure 5. Crystal packing diagram of **2c** down the *c*-axis direction illustrating hydrogen bonding in an hexagonal array as shown with dotted lines. Disordered dichloromethane solvent molecules sit in a 3-fold axis of symmetry.

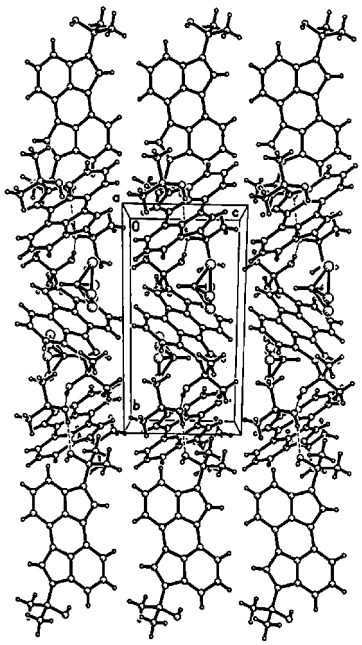

Figure 6. Crystal packing diagram of **2c** down the *a*-axis direction illustrating close packing of layers of cyclopent[*hi*]aceanthrylene molecules.

(Figure 5, view down the *c*-axis). The crystal packing diagram in Figure 6 shows the close contact between layers. The individual layers are held together by a complex hydrogen bonding network between cyclopent[*hi*]aceanthrylene molecules that only translate along the *ab*-plane (Figures 5 and 6). The hexameric hydrogen bonding motif of **2c** gives rise to a relatively broad O−H stretching band at 3431 cm^{-1} and results in the remarkable thermal behavior of **2c**, which remains a solid up to 400 °C.

3. Experimental and Calculated UV−Vis Absorption Spectra. Few reports have been published on the ultraviolet absorption spectral changes associated with going from a polycyclic aromatic hydrocarbon to the introduction of ethynyl substitutents and cyclopentene fusion.[17] The UV−vis spectra of compounds **2a**, **2b**, and **2c** in cyclohexane at ambient

(17) Marsh, N. D.; Mikolajczak, C. J.; Wornat, M. J. *Spectrochim. Acta A* **2000**, *56*, 1499−1511.

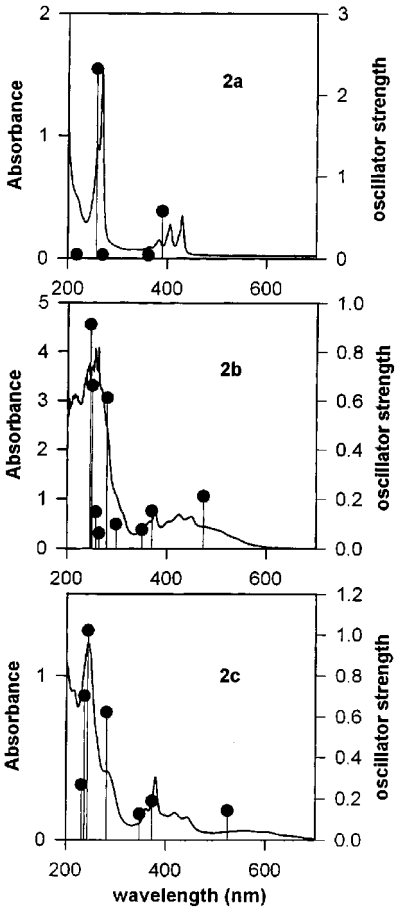

Figure 7. UV-vis absorption spectra for **2a** (top), **2b** (middle), and **2c** (bottom). Characteristic vibrational modes for anthracene derivative **2a**.

temperature are shown in Figure 7. The spectrum of the 9,10-dialkynylanthracene **2a** is substantially red shifted with respect to the spectrum of the unsubstituted anthracene chromophore. An intense absorption at 275 nm is assigned to the B_b transition while the L_a band occurs between 380 and 430 nm with the typical vibrational resolution of the chromophore. With a shift of approximately 50 nm, samples of **2a** possess a pale yellow color as compared to the colorless anthracene. In contrast, crystals and solutions of aceanthrylene **2b** possess a strikingly bright red color. The spectrum of **2b** is characterized by a very strong signal at 260 nm ($\epsilon = 5.05 \times 10^4$ M^{-1} cm^{-1}) and a complex and relatively weaker band system that extends between 300 and 600 nm. The lowest energy transition is a broad band centered at 500 nm ($\epsilon = 4.14 \times 10^3$ M^{-1} cm^{-1}), which has substantial overlap with a set of bands in the 280 to 450 nm region, and which appears to belong to a vibrationally resolved transition. Double cyclopentenelation of the anthracene core to give compound **2c** results in a chromophore with remarkable absorption properties. Crystalline samples of **2c** appear nearly black and dilute solutions reveal a dark green color. The UV absorption spectrum of **2c** possesses three sets of bands in the 200−700 nm region: a strong transition at 245 nm ($\epsilon = 4.31 \times 10^4$ M^{-1} cm^{-1}), a set of maxima between 380 and 420 nm, and a weak and extremely broad transition centered at 570 nm ($\epsilon = 1.84 \times 10^3$ M^{-1} cm^{-1}) that extends from about 500 to 700 nm. These results differ significantly from a previous report by Boere et al.[10d] where only transitions with $\lambda_{max} <$ 443 nm were observed.

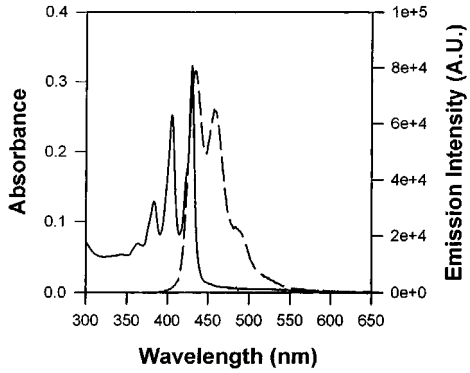

Figure 8. UV−vis absorbance (solid line) of **2a** in methyl cyclohexane. Fluorescence emission (dashed line) of compound **2a** exciting at 377 nm in methyl cyclohexane.

To confirm our observations and to explore the nature of the electronic transitions involved in the spectra of **2a**, **2b**, and **2c**, we carried out semiempirical calculations of their electronic spectra and transition dipole moments. X-ray coordinates were used as the input to calculate optimized geometries using the AM1 method, and the electronic spectra were determined using the ZINDO/S method as implemented by the Hyperchem package with the CI matrix computed with the lowest 201 single excited configurations.[18] The results are illustrated in Figure 7 with bars capped by dark circles indicating the wavelength and oscillator strength of each calculated transition. The overall agreement between calculated and experimental spectra is quite good. The calculations predict the dominance of two band systems assigned to the B_b and L_a transitions in the spectrum of **2a** (Figure 7, top). In agreement with the experimental result, the calculated spectra of **2b** and **2c** are significantly more complex than that of **2a**. Calculations suggest that at least nine transitions with significant oscillator strength contribute to the spectrum of **2b** and seven transitions contribute to that of **2c**. As observed for various nonalternant hydrocarbons, a relatively large energy gap is calculated between S_1 and S_2 in each of the two aceanthrylenes.

4. Fluorescence Emission. The excitation and emission spectra of 9,10-diethynyl anthracene **2a** obtained in cyclohexane are typical of the anthracene chromophore (Figure 8). There is an excellent agreement between the excitation and absorption spectra and there is an excellent mirror symmetry relation between excitation and emission. We determined the fluorescence quantum yield of **2a** using 9,10-diphenyl anthracene as a standard ($\Phi = 0.91$)[19] to obtain a value of $\Phi_F = 0.87$. A monoexponential lifetime for the singlet state was measured by excitation at 405 nm and detection at 435 nm by using time-correlated single photon counting. A relatively small variation observed in lifetime measurements carried out in methyl tetrahydrofuran solutions at 298 and 77 K suggests small contributions from thermal decay. The corresponding lifetimes were 5.8 and 6.3 ns. In contrast to anthracene **2a**, no emission was detected from compounds **2b** and **2c**. Measurements carried out at relatively short wavelengths in search of weak S_2-S_0 fluorescence, prompted by reports of anomalous emission in the case of unsubstituted aceanthrylene,[20] were also negative.

(18) Hypercube, Inc., Gainsville, FL.
(19) Meech, S. R.; Phillip, D. *J. Photochem.* **1983**, *23*, 193−217.
(20) Plummer, B. F.; Al-Saigh, Z. Y.; Arfan, M. *Chem. Phys. Lett.* **1987**, *104*, 389−392.

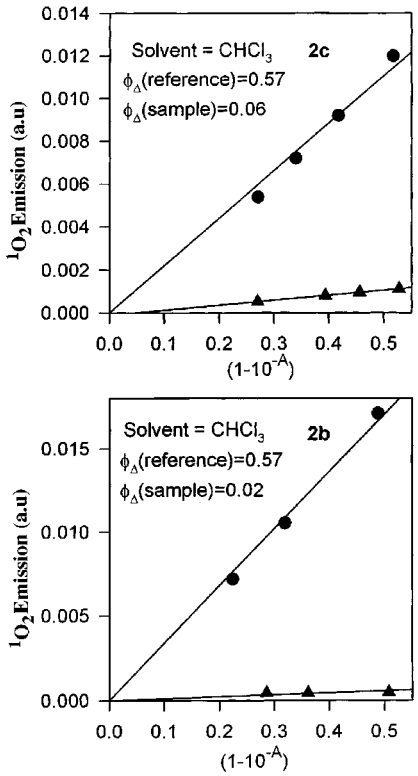

Figure 9. Plots of singlet oxygen yields of **2b** and **2c** (triangles) as a function of absorbed intensity compared with the singlet oxygen yields of 2,2′:5′,2″-terthiophene standard (in filled circles). A = absorbance at λ_{ex} = 366 nm.

Similarly, no emission was observed at 77 K in methylcyclohexane glasses suggesting that fluorescence is not quenched by thermal decay at ambient temperature.

5. $^1O_2$ Quantum Yields. Given the lack of fluorescence from compounds **2b** and **2c**, both at ambient temperature and at 77 K, it seemed likely that their singlet states may decay by intersystem crossing. Attempts to detect the triplet state by phosphorescence emission in either of these compounds by steady state and pulsed excitation were unsuccessful. The relatively low sample stability under conditions of laser flash photolysis experiments has so far prevented us from the direct detection of the triplet state. Thus, in an attempt to establish the formation of the triplet, and in order to determine a possible analogy between the photophysics of compounds **2b** and **2c** with C_{60} and other fullerenes, we decided to carry out an indirect triplet state detection by establishing their efficiency as singlet oxygen ($^1O_2$) sensitizers. Measurements were carried out by detection of $^1O_2$ emission at 1269 nm as a function of increasing sensitizer concentration under conditions where only the triplet state may act as an energy donor.[21] As indicated in Figure 9, quantum yields of $^1O_2$ (Φ_Δ) were measured by comparison of the $^1O_2$ emission signal obtained from **2b** and **2c** to that obtained from 2,2′:5′,2″-terthiophene, which is known to have a Φ_Δ of 0.67.[22] Surprisingly, the values of Φ_Δ obtained in this manner for **2b** and **2c** were 0.02 and 0.06, respectively, which differ substantially from the very efficient triplet state sensitization by fullerenes (Φ_Δ = 1.0 for C_{60}).[9,20]

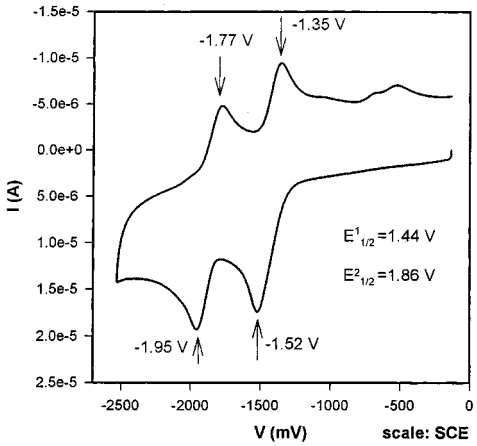

Figure 10. Cyclic voltamogram of cyclopent[*hi*]aceanthrylene **2c** in acetonitrile showing a reversible two-electron reduction.

Since the energetics for sensitization of singlet oxygen should be excellent, the low efficiency of **2b** and **2c** may reflect very low triplet yields, very short triplet lifetimes, or a chemical reaction with molecular oxygen, rather than the expected energy transfer. A very efficient photochemical reaction between **2c** and oxygen was confirmed by irradiation of aerated solutions at ambient temperatures. Decomposition of **2c** into several unidentified products was determined by thin-layer-chromatography and UV−vis absorption measurements. Reaction proceeding at the etheno double bonds is suggested by a change in the UV−vis spectrum as the chromophore of **2c** transforms into the chromophore of aceanthrylene. Further photooxidation results in the evolution of the spectrum from that of aceanthrylene into that of an anthracene chromophore.

6. Cyclic Voltammetry. The chemical and electrochemical reduction of PAHs have a strong correlation with their electronic structure properties. It is well-known that their charge delocalization and distribution reflect well in their NMR properties and chemical reactivity.[23,24] A simple Hückel MO analysis indicates that the HOMO of the aromatic core of **2c** should have energies of $\alpha + 0.57\beta$ and the low-lying nonbonding LUMO should have energy α. By comparison, the aceanthrylene core of **2b** is calculated to have values of $\alpha + 0.52\beta$ and $\alpha - 0.19$ for the HOMO and LUMO levels, respectively. The small HOMO−LUMO gap in the two hydrocarbons is consistent with the low-energy transitions in their UV spectra. The low LUMO levels predict a very facile two-electron reduction in the case of **2c**. Although the two-electron chemical reduction of the parent aceanthrylene has been analyzed in some detail,[25] attempts to measure the electrochemical reduction of the alkynyl-containing aceanthrylene **2b** were unsuccessful as it decomposed readily under the conditions of cyclic voltammetry measurements. In contrast, the cyclic voltammogram of **2c** obtained with a scanning rate of 50 mV/s at ambient temperature with Bu_4NPF_6 in MeCN reveals the predicted behavior (Figure 10). We were able to record two well-resolved reduction waves with $E^1_{1/2} = -1.44$ V and $E^2_{1/2} = -1.86$ V vs SCE. The first reduction wave of **2c** is significantly lower than that of anthracene (−1.95 V vs SCE) and perylene (−1.67 vs SCE)

(21) Foote, C. S.; Clennan, E. L. *Active Oxygen in Chemistry*; Foote, C. S., Valentine, J. S., Greenberg, A., Liebman, J. F., Eds.; Blackie Academic and Professional: New York, 1995.
(22) Wilkinson, F.; Helman, W. P.; Ross, A. B. *J. Phys. Chem. Ref. Data* **1993**, *22*, 113−131.
(23) Benshafrut, R.; Shabtai, E.; Rabinovitz, M.; Scott, L. T. *Eur. J. Org. Chem.* **2000**, *7*, 1091−1106.
(24) Müllen, K. *Chem. Rev.* **1984**, *84*, 603−646.
(25) Rabideau, P. W.; Mooney, J. L.; Kimmer Smith, W.; Sygula, A. *J. Org. Chem.* **1988**, *53*, 589−591.

Scheme 4

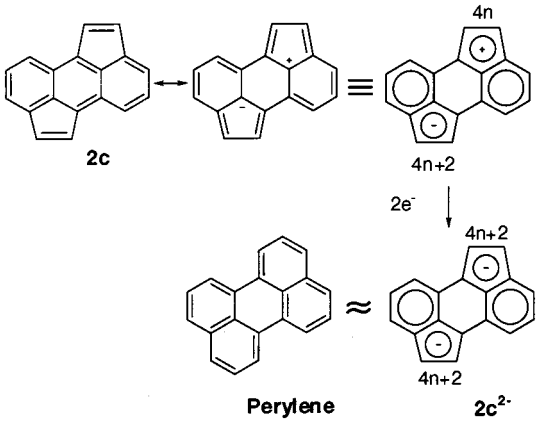

and it is only slightly higher than that of C_{60} (−1.41 V vs SCE). The facile reduction of **2c** can be visualized by analysis of resonance forms invoking delocalization of the π-electrons from the etheno bridge. As indicated in Scheme 4, such delocalization would give resonance structures consisting of an aromatic 10e$^-$ benzocyclopentadienyl anion and an antiaromatic 8e$^-$ benzocyclopentadienyl cation. A two-electron reduction of **2c** gives rise to two stabilized aromatic benzocyclopentadienyl anions in **2c**$^{2-}$, with a structure that is analogous to that of perylene.

Conclusions

The Pd(0)-catalyzed synthesis of nonalternant CP-PAHs from aryl halides and terminal acetylenes is a promising method for the preparation of these interesting compounds. A loose analogy between the properties of **2c** and C_{60} suggests that the properties of the latter may be determined more by its being a nonalternant CP-PAH than by its curved surface and three-dimensional closed π-electron topology. It is of interest to note that cyclopent[*hi*]-aceanthrylene **2c** with 18 total electrons is formally a Hückel aromatic system. However, bond lengths and small diatropic shifts suggest a structure consisting of an anthracene core (14 electrons) and two isolated double bonds. In contrast, the dianion **2c**$^{2-}$ (Scheme 4) with 20 electrons and formally antiaromatic may be well represented by two aromatic benzocyclopentadienyl units.

Experimental Section

Materials and Methods. All starting materials were of reagent grade and used without further purification. Solvents for reaction and photophysical measurements were either distilled or of spectroscopic grade. ^{1}H and ^{13}C NMR spectra were obtained on an AMS 360 (360 MHz), Bruker ARX400 (400 MHz), or Avance Bruker ARX500 (500 MHz) spectrometer. ^{1}H and ^{13}C NMR spectra were obtained in acetone-d_6 with TMS as an internal standard, unless otherwise noted. X-ray data were taken on a Bruker Smart 1K X-ray diffractometer equipped with a large area CCD detector. Structure solution and refinement were conducted using a SHELXTL package from Bruker. IR spectra were obtained on a Perkin-Elmer Paragon 1000 FT-IR spectrometer. UV−vis spectra were acquired on a HP 8453 spectrometer. High-resolution electron impact (EI-HiRes) mass spectra were obtained on a VG Autospec (Micromass, Beverly, MA) spectrometer. Melting points were determined with a MEL-TEMP II apparatus equipped with a Fluke 50S K/J thermometer. Column chromatography was performed with silica gel (40 μm, 32−63 μm, Scientific Absorbents Incorporated).

Preparation of PAH 2a, CP-PAHs 2b and 2c. A mixture of 9,10-dibromoanthracene (0.52 g, 1.547 mmol), $Pd(PPh_3)_2Cl_2$ (0.047 g, 0.067 mmol), PPh_3 (0.098 g, 0.374 mmol), and $CuSO_4/Al_2O_3$ (0.082 g, 0.514 mmol) was suspended in 25 mL of deoxygenated benzene in a 50-mL three-necked round-bottom flask equipped with a magnetic stir bar and water condenser. Et_3N (0.610 g, 6.027 mmol) and 2-methyl-3-butyn-2-ol (0.503 g, 5.985 mmol) were added to the suspension in one portion. The reaction was refluxed for ca. 16 h and quenched with NH_4Cl after all of the 9,10-dibromoanthracene had reacted. The biphasic mixture was separated and the aqueous layer was extracted three times with Et_2O. The combined organic layers were dried over $MgSO_4$, filtered, and concentrated in vacuo to give a crude mixture of **2a**, **2b**, and **2c**. The isomers were purified by flash chromatography (Chromatoflash) with hexanes and ethyl acetate (3:1, v/v) to give 0.413 g of **2a**, **2b**, and **2c**. After chromatography, 73 mg of **2a**, 120 mg of **2b**, and 100 mg of **2c** were obtained and used for characterization, X-ray analyses, and photophysical measurements. Detailed X-ray data tables for **2a**, **2b**, and **2c** are included as Supporting Information.

2a: Yellow-orange prisms; mp 214−217.5 °C; ^{1}H NMR (500 MHz, acetone-d_6) δ 8.59 (dd, J = 6.7, 3.3 Hz, 4H), 7.67 (dd, J = 6.7, 3.3 Hz, 4H), 4.89 (s, 2H, OH), 1.79 (s, 12H); ^{13}C NMR (125 MHz, acetone-d_6) δ 132.64, 127.80, 118.88, 109.63, 85.58, 78.06, 65.76, 32.12; FT-IR (KBr, cm^{-1}) 3362, 3300, 3061, 2978, 2926, 2218, 1619, 1518, 1436, 1392, 1224, 1164, 1141, 950, 761, 642; UV−vis (solvent: dichloromethane) λ_{max}(nm) 260, 270, 365, 385, 407, 432; HRMS (EI) m/z (M$^+$) calcd for $C_{24}H_{22}O_2$ 342.1620, obsd 342.1616.

2b: Dark-red prisms; mp 172−174.5 °C; ^{1}H NMR (500 MHz, acetone-d_6) δ 8.58 (d, J = 8.6 Hz, 1H), 8.34 (d, J = 8.5 Hz, 1H), 8.28 (d, J = 8.5 Hz, 1H), 8.16 (d, J = 6.6 Hz, 1H), 7.69−7.62 (m, 2H), 7.60−7.57 (m, 1H), 7.45 (s, 1H), 4.91 (s, 1H, OH), 4.30 (s, 1H, OH), 1.78 (s, 6H), 1.76 (s, 6H); ^{13}C NMR (125 MHz, acetone-d_6) δ 153.13, 140.27, 135.77, 135.44, 129.16, 128.99, 128.81, 128.68, 128.32, 128.05, 127.06, 126.87, 126.84, 125.51, 121.48, 119.12, 108.91, 78.24, 71.18, 65.75, 32.17, 32.07; FT-IR (KBr, cm^{-1}) 3437, 3063, 2978, 2931, 2867, 2206, 1516, 1454, 1438, 1396, 1227, 1166, 955, 759; UV−vis (solvent: methylcyclohexane) λ_{max}(nm) 376, 405, 425, 450; HRMS (EI) m/z (M$^+$) calcd for $C_{24}H_{22}O_2$ 342.1620, obsd 342.1615.

2c: Black hexagonal prisms; mp >400 °C dec; ^{1}H NMR (500 MHz, acetone-d_6) δ 8.26 (d, J = 8.5 Hz, 2H), 8.19 (d, J = 6.6 Hz, 2H), 7.71 (dd, J = 8.5, 6.7 Hz, 2H), 7.45 (s, 2H), 4.26 (s, 2H, OH), 1.77 (s, 12H); ^{13}C NMR (125 MHz, acetone-d_6) δ 152.55, 140.59, 136.84, 129.53, 129.23, 127.86, 125.86, 124.94, 121.39, 71.24, 32.21; FT-IR (KBr, cm^{-1}) 3277, 3060, 2968, 2930, 1522, 14.98, 1441, 1409, 1376, 1358, 1164, 940, 794; UV−vis (solvent: methylcyclohexane) λ_{max}(nm) 246, 361, 380, 417, 447, 522, 592, 660; HRMS (EI) m/z (M$^+$) calcd for $C_{24}H_{22}O_2$ 342.1620, obsd 342.1614.

X-ray Structure Determination. X-ray quality single crystals of compounds **2a**, **2b**, and **2c** ($C_{24}H_{22}O_2$) were grown by slow evaporation from chloroform, benzene, and methylene chloride, respectively. A prism with approximate dimensions was used for X-ray crystallographic analysis. The X-ray intensity data were measured at either 298 or 100 K on a Bruker SMART 1000 CCD-based X-ray diffractometer system equipped with a Mo-target X-ray tube (λ = 0.71073 Å) operated at 2250 W power. The detector was placed at a distance of 4.986 cm from the crystal. A total of 1321 frames were collected with a scan width of 0.3° in ω, with an exposure time of 30 s/frame. The total data collection time was ca. 18 h. The frames were integrated with the Bruker SAINT software package using a narrow-frame integration algorithm. Analysis of the data showed negligible decay during data collection. The structure was refined based on the respective space groups, using the Bruker SHELXTL (Version 5.3) Software Package.

UV−Vis and Steady-State Fluorescence Spectra. Absorption spectra were obtained with a Hewlett-Packard 8453 spectrophotometer. Fluorescence spectra were recorded with a Spex-Fluorolog II spectrofluorometer and corrected for nonlinear instrumental response. The fluorescence quantum yield of **2a** was measured with 9,10-diphenylanthracene in cyclohexane as a reference.

Time-Resolved Fluorescence Decays. The fluorescence decays were measured with a time-correlated single photon count fluorimeter

(Edinburgh Instruments, Model FL900CDT) equipped with a pulsed H_2 discharge lamp operating at 0.4 bar. When necessary, the fluorescence intensity was attenuated to obtain an average number of detected fluorescence photons lower than 1% of the excitation source repetition rate (40 kHz). The experimentally measured luminescent emission was deconvoluted from the instrumental response to obtain the decay. The instrumental response was measured by using a LUDOX suspension as a scattering sample, setting both monochromators at the emission wavelength of the sample. To eliminate polarization effects, measurements at 77 K were carried out exciting the sample with vertically polarized light and setting the emission polarizer at the magic angle.

Semiempirical Calculations. The geometries of the molecules were optimized using the AM1 method, and the electronic spectrum and transition moment directions were computed using the ZINDO/S method as implemented in the Hyperchem package.[18] The CI matrix was computed using 201 lowest, single excited configurations.

Singlet Oxygen Quantum Yield. Singlet oxygen quantum yields were determined by using the Ge photodiode to observe the 1268-nm emission of $^1O_2$. Air-saturated chloroform samples were excited at 355 nm. A silicon cutoff filter at 1100 nm and a 1270 nm interference filter were used to eliminate the fluorescence from the sample and scattered laser light. Collection of the data was done at a 90° angle to the laser beam and was enhanced by addition of a parabolic mirror at a 270° angle. The production of $^1O_2$ by the sample was evaluated from the phosphorescence of singlet oxygen at 1268 nm. For each compound, four samples with different absorbances ($A = 0.05-0.4$) were prepared and the intensity of singlet oxygen emission measured. The observed intensity is linear with the absorbed intensity of the samples, and the ratio of the slopes of the plots is proportional to the ratio of singlet oxygen quantum yields. α-Terthienyl (2,2′:5′,2″-terthiophene) was used as the primary reference ($\phi_\Delta = 0.67$).

Cyclic Voltammetry. Cyclic voltammetry was performed on a BAS 100B Electrochemical Analyzer equipped with a three-electrode cell in a solution of 0.1 M tetrabutylammonium hexafluorophosphate (Bu_4NPF_6) dissolved in acetonitrile at a scan rate of 50 mV/s. Compound **2c** was dissolved in THF and the reduction potential measured. A Pt wire was used as the counter electrode and an $Ag/AgNO_3$ (0.1 M) solution was used as the reference electrode. The potential was corrected with a saturated calomel electrode (SCE) by measuring the ferrocene/ferrocenium couple in the system (0.31 V versus SCE).

Acknowledgment. This work was supported by the National Science Foundation (grants DMR9988439, CHE0073431, and CHE9871332 for X-ray diffractometer). We thank Dr. Saeed Khan for advice on the solution and refinement of **2a**, **2b**, and **2c**.

Supporting Information Available: X-ray data tables and structures for **2a**, **2b**, and **2c** (PDF). This material is available free of charge via the Internet at http://pubs.acs.org.

JA016189B